remarkable that the two processes proceed along such dissimilar pathways when their kinetic characteristics and the structural features of the two anions show such close resemblances.

Our interpretation of the NMR data as indicating O-protonation of II is confirmed by the isotopic evidence. The N-protonation observed for I remains unique among oxoanions, and the more conventional behavior of the closely related anion II suggests that a close energetic balance is probably involved. An ab initio calculation by Cremaschi and Whitten,[19] using crystal lattice geometry and dimensions,[20] shows that the isolated $HN_2O_3^-$ anion protonated at its nitroso-like O atom should be more stable than the N_1-protonated form by about 52 kJ mol^{-1}. Any energetic accounting for the N-protonation of this species observed in solution may therefore require that a heavy burden be placed upon distortion and solvent effects, and it is interesting to note that this price is apparently not paid in the more symmetrical case of hyponitrite.

Registry No. $Na_2N_2O_2$, 60884-93-7; $Na_2N_2O_3$, 13826-64-7; $N_2O_2^{2-}$, 15435-66-2.

(19) Cremaschi, P.; Whitten, J. L., private communication.

(20) Hope, H.; Sequeira, M. R. *Inorg. Chem.* **1973**, *12*, 286.
(21) Witanowski, M.: Stefeniek, L.: Szymanski, S.: Januszewski, H. *J. Magn. Reson.* **1977**, *28*, 217.
(22) AEI MS-30, Stony Brook Mass Spectrometry Facility.

Contribution from the Departments of Chemistry, University of Illinois at Chicago, Chicago, Illinois 60680, and University of Virginia, Charlottesville, Virginia 22901, and the Kamerlingh Onnes Laboratory of the University of Leiden, Leiden, The Netherlands

Magnetic Ordering in $CoCl_2 \cdot 2P(C_6H_5)_3$ and $CoBr_2 \cdot 2P(C_6H_5)_3$

RICHARD L. CARLIN,*[1] ROBERT D. CHIRICO,[1] EKK SINN,*[2] G. MENNENGA,[3] and L. J. DE JONGH*[3]

Received December 8, 1981

The crystal structures of $CoCl_2 \cdot 2P(C_6H_5)_3$ and $CoBr_2 \cdot 2P(C_6H_5)_3$ are reported. Both crystals belong to the space group $P2/c$ with $Z = 2$: for the chloride, $a = 11.764$ (2) Å, $b = 8.250$ (3) Å, $c = 17.254$ (7) Å, and $\beta = 106.57$ (4)°; for the isostructural bromide, $a = 11.828$ (2) Å, $b = 8.325$ (2) Å, $c = 17.365$ (5) Å, and $\beta = 106.58$ (3)°. The crystal susceptibilities of the compounds have been measured over the temperature interval 40 mK–4 K. Antiferromagnetic ordering is observed at 0.21 ± 0.01 K (Cl) and 0.25 ± 0.01 K (Br). The specific heats have also been measured, and the ordering has been confirmed. Both compounds order with lattice dimensionality between 1 and 2, and all the data may be fit by a theoretical calculation for the rectangular Ising lattice, with $J_x/J_y = 0.31 \pm 0.02$ for the chloride and 0.10 ± 0.02 for the bromide. These results require that the $|\pm^3/_2\rangle$ component of the $^4A_2$ level be the ground state in both systems.

Introduction

The nature of the ground state of tetrahedral cobalt(II) complexes continues to be a problem of interest.[4-9] The determination of the sign and magnitude of the zero-field splitting of the $CoCl_4^{2-}$ ion in several lattices has attracted widespread attention as has also the concomitant magnetic ordering. We note that the tetrahedral ion in Cs_3CoCl_5, for example, exhibits a large zero-field splitting of about 10 K and the compound orders according to the three-dimensional Ising model.[10] On the other hand, the zero-field splitting in Cs_2CoCl_4 is 13.5 ± 1 K,[5,6] but it is of opposite sign to that in Cs_3CoCl_5. This leads to an anisotropy in the magnetic interaction according to the magnetic XY model.[5-7] This system is of further interest because it behaves as a linear-chain magnet.[5-7,11]

We report here a study of the compounds CoX_2L_2 where X is chloride or bromide and L is triphenylphosphine, $P(C_6H_5)_3$. Previous work on these compounds is limited to powder susceptibilities at high temperatures,[12] to polarized crystal spectra,[13] and to paramagnetic anisotropy measurements at 25 °C[14] and down to 20 K.[15] The crystal structures of both compounds have now been determined, and single-crystal susceptibility and specific heat measurements at low temperatures are reported. These measurements determine the sign of the zero-field splitting (ZFS) of the $^4A_2$ ground state without ambiguity, but the measurements are at temperatures too low to allow the determination of the magnitude of the ZFS. The results are also of interest because they indicate that antiferromagnetic ordering of reduced lattice dimensionality occurs in both salts.

Experimental Section

Single crystals of each material were grown from warm ethanol and oriented by means of the known morphology.[15] Susceptibilities were measured by an ac mutual-inductance technique at near zero field. Temperatures below 1 K were obtained by means of a ^3He–^4He dilution refrigerator; the experimental procedure has been reported

(1) University of Illinois at Chicago.
(2) University of Virginia.
(3) University of Leiden.
(4) Carlin, R. L. *Transition Met. Chem.* **1965**, *1*, 1.
(5) Algra, H. A.; de Jongh, L. J.; Blöte, H. W. J.; Huiskamp, W. J.; Carlin, R. L. *Physica B+C (Amsterdam)* **1976**, *82B+C*, 239.
(6) McElearney, J. N.; Merchant, S.; Shankle, G. E.; Carlin, R. L. *J. Chem. Phys.* **1977**, *66*, 450.
(7) Smit, J. J.; de Jongh, L. J. *Physica B+C (Amsterdam)* **1979**, *97B+C*, 224.
(8) Figgis, B. N.; Mason, R.; Smith, A. R. P.; Williams, G. A. *Acta Crystallogr., Sect. B* **1980**, *B36*, 509.
(9) Carlin, R. L. *J. Appl. Phys.* **1981**, *52*, 1993.
(10) Wielinga, R. F.; Blöte, H. W. J.; Roest, J. A.; Huiskamp, W. J. *Physica (Amsterdam)* **1967**, *34*, 223.
(11) Duxbury, P. M.; Oitmaa, J.; Barber, M. N.; van der Bilt, A.; Joung, K. O.; Carlin, R. L. Phys. Rev *B: Condens. Mater* **1981**, *24*, 5149.
(12) Cotton, F. A.; Faut, O. D.; Goodgame, D. M. L.; Holm, R. H. *J. Am. Chem. Soc.* **1961**, *83*, 1780.
(13) Simo, C.; Holt, S. L. *Inorg. Chem.* **1968**, *7*, 2655.
(14) Horrocks, W. De W., Jr.; Greenberg, E. S. *Inorg. Chem.* **1971**, *10*, 2190.
(15) Davies, J. E.; Gerloch, M.; Phillips, D. J. *J. Chem. Soc., Dalton Trans.* **1979**, 1836.

0020-1669/82/1321-2218$01.25/0

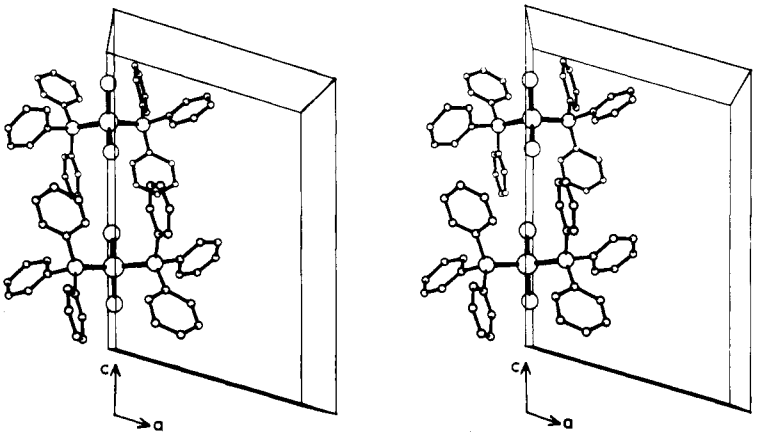

Figure 1. Stereopair view of $CoCl_2 \cdot 2P(C_6H_5)_3$.

in detail.[16,17] The specific heats were measured in an adiabatic demagnetization apparatus similar to that described elsewhere.[18]

Crystal Data and Data Collection. $CoCl_2P_2C_{36}H_{30}$: mol wt 654, space group $P2/c$, $Z = 2$, $a = 11.764$ (2) Å, $b = 8.250$ (3) Å, $c = 17.254$ (7) Å, $\beta = 106.57$ (4)°, $V = 1605$ Å^3, $\rho_{calcd} = 1.35$ g cm^{-3}, $\rho_{obsd} = 1.33$ g cm^{-3}, μ(Mo Kα) = 8.5 cm^{-1}; crystal dimensions (distances in mm of faces from centroid) (100) 0.16, ($\bar{1}$00) 0.16, (010) 0.47, (0$\bar{1}$0) 0.47, (001) 0.52, (00$\bar{1}$) 0.52; maximum and minimum transmission coefficients 0.82, 0.54. $CoBr_2P_2C_{36}H_{30}$: mol wt 743, space group $P2/c$, $Z = 2$, $a = 11.828$ (2) Å, $b = 8.325$ (2) Å, $c = 17.365$ (5) Å, $\beta = 106.58$ (3)°, $V = 1639$ Å^3, $\rho_{calcd} = 1.51$ g cm^{-3}, $\rho_{obsd} = 1.48$ g cm^{-3}, μ(Mo Kα) = 32.5 cm^{-1}; crystal dimensions (mm from centroid) (100) 0.19, ($\bar{1}$00) 0.19, (010) 0.31, (0$\bar{1}$0) 0.31, (001) 0.25, (00$\bar{1}$) 0.25, (10$\bar{2}$) 0.25, ($\bar{1}$02) 0.25; maximum and minimum transmission coefficients 0.51, 0.24.

Cell dimensions and space-group data were obtained by standard methods on an Enraf-Nonius four-circle CAD-4 diffractometer. The θ–2θ scan technique was used, as previously described,[19] to record the intensities for all nonequivalent reflections for which $1° < 2\theta < 50°$ for $CoCl_2 \cdot 2P(C_6H_5)_3$ and $1° < 2\theta < 48°$ for $CoBr_2 \cdot 2P(C_6H_5)_3$. Scan widths were calculated as $A + B \tan \theta$, where A is estimated from the mosaicity of the crystal and B allows for the increase in width of peak due to $K\alpha_1$–$K\alpha_2$ splitting. The values of A and B were 0.60 and 0.30°, respectively.

The intensities of four standard reflections, monitored regularly, showed no greater fluctuations than those expected from Poisson statistics. The raw intensity data were corrected for Lorentz–polarization effects and absorption. Of the 2682 and 2313 independent intensities for $CoCl_2 \cdot 2P(C_6H_5)_3$ and $CoBr_2 \cdot 2P(C_6H_5)_3$, respectively, 2483 and 1872 had $F_o^2 > 3\sigma(F_o^2)$, where $\sigma(F_o^2)$ was estimated from counting statistics.[20] These data were used in the final refinement of the structural parameters.

Structure Determination. The position of the cobalt atom in $CoCl_2 \cdot 2P(C_6H_5)_3$ was determined from a three-dimensional Patterson function and then placed at 0, 0.2, 0.25 (x, z fixed). This position imposed crystallographic symmetry on the molecule. The intensity data were phased sufficiently well by these positional coordinates to permit location of the other nonhydrogen atoms from Fourier syntheses. Full-matrix least-squares refinement was carried out as previously described.[19] Anisotropic temperature factors were then introduced for all nonhydrogen atoms. Further Fourier difference functions permitted location of the hydrogen atoms, which were included in the refinement for three cycles of least-squares and then held fixed. Refinement of the $CoBr_2 \cdot 2P(C_6H_5)_3$ data was carried out similarly, with use of the atomic coordinates for the chloride as starting values. The model converged with $R = 4.2\%$ and $R_w = 4.9\%$ for the chloride and $R = 5.3\%$ and $R_w = 5.5\%$ for the bromide. A final Fourier difference function was featureless. Tables of the observed and calculated structure factors are available.[21] The principal programs used are as previously described.[19]

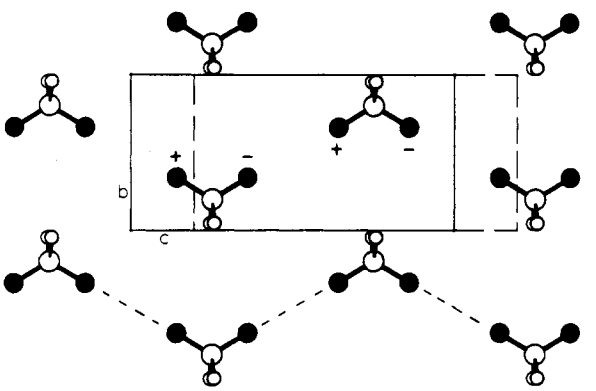

Figure 2. Perspective view of the molecular packing projected onto the bc plane. The halide ions (filled circles) lie 0.059 Å above (+) or 0.059 Å below (−) the plane. The phenyl rings are omitted for clarity.

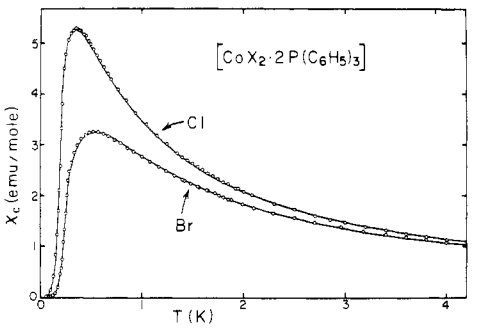

Figure 3. Susceptibilities parallel to the c axis of $CoCl_2 \cdot 2P(C_6H_5)_3$ and of $CoBr_2 \cdot 2P(C_6H_5)_3$. The data points are experimental, and the fitted curves are described in the text.

Results

Final positional and thermal parameters for both compounds are given in Table I. Tables II and III contain the bond lengths and angles. The digits in parentheses in the tables are the estimated standard deviations in the least significant figures quoted and were derived from the inverse matrix in the course of least-squares refinement calculations. Figure 1 is a stereopair view of the molecule, and Figure 2 is the molecular packing projected on the bc plane. The structure consists of well-separated molecules (Figure 2), the closest intermolecular approaches being a phenyl carbon atom (C15) and Cl (3.550 Å) or Br (3.591 Å) atom of a neighboring molecule. The

(16) van der Bilt, A.; Joung, K. O.; Carlin, R. L.; de Jongh, L. J. *Phys. Rev. B: Condens. Matter* **1980**, *22*, 1259.
(17) Chirico, R. D.; Carlin, R. L. *Inorg. Chem.* **1980**, *19*, 3031.
(18) Algra, H. A.; de Jongh, L. J.; Huiskamp, W. J.; Carlin, R. L. *Physica B+C (Amsterdam)* **1977**, *92B+C*, 187.
(19) Joung, K. O.; O'Connor, C. J.; Sinn, E.; Carlin, R. L. *Inorg. Chem.* **1979**, *18*, 804.
(20) O'Connor, C. J.; Sinn, E.; Carlin, R. L. *Inorg. Chem.* **1977**, *16*, 3314.
(21) Supplementary material.

Table I. Positional and Thermal Parameters and Their Estimated Standard Deviations[a]

(A) $CoCl_2 \cdot 2P(C_6H_5)_3$

atom	x	y	z	B_{11}	B_{22}	B_{33}	B_{12}	B_{13}	B_{23}
Co	0.0000 (0)	0.19892 (7)	0.2500 (0)	3.48 (2)	3.44 (2)	4.01 (2)	−0.0516 (0)	1.61 (2)	−0.0450 (0)
Cl	0.00500 (8)	0.3385 (1)	0.14153 (6)	6.19 (4)	5.35 (4)	5.90 (4)	0.30 (3)	2.68 (3)	1.84 (3)
P	0.17889 (7)	0.0455 (1)	0.29152 (5)	3.20 (3)	3.55 (3)	3.64 (3)	−0.08 (2)	1.17 (2)	−0.13 (3)
C(11)	0.1842 (3)	−0.0973 (4)	0.3731 (2)	3.3 (1)	3.6 (1)	3.6 (1)	−0.5 (1)	0.87 (9)	0.0 (1)
C(12)	0.1511 (3)	−0.0412 (4)	0.4397 (2)	5.1 (1)	4.7 (2)	4.3 (1)	0.2 (1)	1.80 (10)	−0.2 (1)
C(13)	0.1494 (3)	−0.1452 (5)	0.5022 (2)	5.7 (2)	6.0 (2)	3.8 (1)	−0.4 (1)	1.55 (12)	0.3 (1)
C(14)	0.1820 (3)	−0.3058 (5)	0.4987 (2)	5.0 (1)	5.6 (2)	4.5 (1)	−0.9 (1)	1.24 (12)	1.0 (1)
C(15)	0.2152 (3)	−0.3618 (4)	0.4345 (2)	6.0 (2)	4.2 (1)	5.5 (2)	0.3 (1)	1.52 (13)	0.7 (1)
C(16)	0.2171 (3)	−0.2592 (4)	0.3705 (2)	5.0 (1)	4.4 (1)	4.6 (1)	0.4 (1)	1.73 (11)	0.2 (1)
C(21)	0.2188 (3)	−0.0739 (4)	0.2140 (2)	3.5 (1)	3.6 (1)	3.9 (1)	0.4 (1)	1.27 (9)	0.3 (1)
C(22)	0.1370 (3)	−0.1800 (4)	0.1672 (2)	3.9 (1)	4.2 (1)	4.9 (1)	0.4 (1)	1.28 (11)	−0.4 (1)
C(23)	0.1637 (3)	−0.2703 (5)	0.1072 (2)	5.6 (2)	4.4 (2)	5.6 (2)	0.5 (1)	0.87 (14)	−1.0 (1)
C(24)	0.2715 (3)	−0.2557 (5)	0.0931 (2)	6.1 (2)	5.0 (2)	4.7 (1)	0.9 (1)	1.98 (11)	−1.1 (1)
C(25)	0.3548 (3)	−0.1500 (5)	0.1389 (2)	5.2 (1)	6.8 (2)	7.0 (2)	−0.2 (1)	3.70 (10)	−1.4 (2)
C(26)	0.3293 (3)	−0.0579 (5)	0.1992 (2)	3.9 (1)	5.3 (2)	5.2 (1)	−0.4 (1)	1.61 (11)	−1.1 (1)
C(31)	0.3038 (3)	0.1823 (4)	0.3315 (2)	4.0 (1)	3.8 (1)	4.7 (1)	−0.5 (1)	2.08 (9)	−0.8 (1)
C(32)	0.3083 (3)	0.3240 (4)	0.2889 (2)	4.7 (1)	4.6 (2)	6.2 (2)	−0.3 (1)	1.91 (12)	0.1 (1)
C(33)	0.4048 (3)	0.4292 (5)	0.3163 (3)	5.5 (1)	5.1 (2)	10.0 (2)	−1.5 (1)	3.91 (14)	−0.4 (2)
C(34)	0.4914 (4)	0.3941 (6)	0.3843 (3)	5.6 (2)	7.3 (2)	10.9 (3)	−3.0 (2)	2.41 (19)	−2.0 (2)
C(35)	0.4870 (4)	0.2535 (7)	0.4275 (3)	5.5 (2)	8.6 (3)	8.7 (3)	−2.5 (2)	0.14 (20)	−0.3 (3)
C(36)	0.3927 (3)	0.1481 (5)	0.4006 (3)	4.6 (2)	6.6 (2)	5.4 (2)	−1.2 (2)	0.33 (14)	0.1 (2)

atom	x	y	z	B, Å²	atom	x	y	z	B, Å²
H(12)	0.109 (8)	0.065 (11)	0.443 (5)	4 (2)	H(25)	0.442 (8)	−0.119 (12)	0.132 (6)	5 (2)
H(13)	0.148 (9)	−0.112 (13)	0.550 (6)	7 (3)	H(26)	0.384 (9)	0.025 (11)	0.229 (6)	5 (2)
H(14)	0.153 (8)	−0.353 (12)	0.535 (6)	6 (2)	H(32)	0.251 (7)	0.356 (11)	0.250 (5)	4 (2)
H(15)	0.264 (8)	−0.475 (11)	0.445 (6)	5 (2)	H(33)	0.415 (9)	0.534 (12)	0.290 (6)	7 (3)
H(16)	0.242 (7)	−0.304 (9)	0.317 (5)	3 (2)	H(34)	0.553 (7)	0.474 (11)	0.399 (5)	4 (2)
H(22)	0.049 (9)	−0.193 (11)	0.183 (6)	5 (2)	H(35)	0.569 (9)	0.226 (13)	0.473 (6)	7 (3)
H(23)	0.099 (7)	−0.345 (10)	0.068 (6)	5 (2)	H(36)	0.400 (8)	0.019 (11)	0.422 (6)	5 (2)
H(24)	0.289 (8)	−0.317 (11)	0.056 (5)	5 (2)					

(B) $CoBr_2 \cdot 2P(C_6H_5)_3$

atom	x	y	z	B_{11}	B_{22}	B_{33}	B_{12}	B_{13}	B_{23}
Br	0.00350 (7)	0.34458 (9)	0.13644 (5)	6.32 (4)	5.31 (4)	6.42 (3)	0.33 (3)	2.43 (3)	1.83 (3)
Co	0.0000 (0)	0.1934 (1)	0.2500 (0)	3.57 (5)	3.52 (5)	4.51 (5)	0.0000 (0)	1.45 (4)	0.0000 (0)
P	−0.1796 (1)	0.0447 (2)	0.1097 (1)	3.34 (7)	3.44 (7)	4.48 (7)	0.13 (6)	1.00 (6)	0.14 (6)
C(11)	−0.1889 (5)	−0.0985 (8)	0.1289 (4)	3.0 (2)	4.0 (3)	3.8 (3)	0.1 (2)	0.5 (2)	0.1 (2)
C(12)	−0.1547 (7)	−0.0487 (8)	0.0632 (4)	6.0 (4)	4.1 (3)	5.6 (3)	−0.2 (3)	1.2 (3)	0.1 (3)
C(13)	−0.1589 (6)	−0.1517 (9)	0.0000 (4)	5.4 (3)	5.6 (4)	5.0 (3)	0.3 (3)	1.6 (3)	0.3 (3)
C(14)	−0.1923 (7)	−0.3078 (9)	0.0040 (4)	5.3 (3)	5.2 (3)	5.1 (3)	0.5 (3)	0.8 (3)	−0.9 (3)
C(15)	−0.2246 (7)	−0.3596 (8)	0.0700 (5)	5.8 (4)	4.1 (3)	6.9 (4)	0.1 (3)	1.4 (3)	−0.6 (3)
C(16)	−0.2246 (6)	−0.2569 (8)	0.1323 (4)	4.8 (3)	4.1 (3)	5.0 (3)	−0.1 (3)	0.9 (3)	0.5 (3)
C(21)	−0.2199 (5)	−0.0698 (7)	0.2870 (4)	3.3 (3)	3.7 (3)	4.5 (3)	−0.4 (2)	0.9 (2)	−0.2 (2)
C(22)	−0.1368 (6)	−0.1704 (8)	0.3355 (4)	4.3 (3)	4.7 (3)	5.3 (3)	−0.2 (3)	1.3 (2)	0.1 (3)
C(23)	−0.1634 (7)	−0.2613 (9)	0.3961 (4)	5.9 (4)	3.8 (3)	5.6 (3)	0.3 (3)	0.9 (3)	1.2 (3)
C(24)	−0.2707 (6)	−0.2490 (9)	0.4082 (4)	5.8 (4)	4.6 (3)	5.7 (3)	−0.7 (3)	1.8 (3)	1.5 (3)
C(25)	−0.3554 (7)	−0.1490 (9)	0.3606 (5)	6.0 (3)	6.9 (4)	7.7 (4)	−0.4 (3)	3.6 (3)	1.3 (3)
C(26)	−0.3292 (6)	−0.0582 (9)	0.3011 (4)	4.1 (3)	5.2 (4)	6.9 (4)	0.5 (3)	1.8 (3)	1.4 (3)
C(31)	−0.3032 (5)	0.1814 (8)	0.1705 (4)	3.5 (3)	4.0 (3)	5.3 (3)	0.5 (2)	1.4 (2)	1.2 (3)
C(32)	−0.3088 (6)	0.3202 (8)	0.2127 (5)	5.1 (3)	4.3 (3)	6.8 (4)	0.5 (3)	1.9 (3)	0.2 (3)
C(33)	−0.4050 (7)	0.4224 (10)	0.1865 (5)	6.8 (4)	4.8 (4)	11.0 (5)	1.5 (3)	4.4 (3)	1.4 (4)
C(34)	−0.4891 (7)	0.3881 (12)	0.1152 (6)	3.8 (3)	8.5 (5)	10.2 (6)	2.3 (4)	0.4 (4)	2.6 (4)
C(35)	−0.4860 (9)	0.2506 (12)	0.0740 (6)	8.5 (5)	8.2 (5)	7.6 (5)	3.9 (4)	−0.5 (4)	0.4 (5)
C(36)	−0.3098 (7)	0.1489 (9)	0.0989 (5)	4.6 (4)	5.4 (4)	7.0 (4)	1.1 (3)	−0.2 (3)	0.4 (4)

atom	x	y	z	B, Å²	atom	x	y	z	B, Å²
H(12)	−0.139 (9)	0.04 (1)	0.053 (6)	6 (3)	H(25)	−0.418 (9)	−0.12 (1)	0.386 (5)	5 (3)
H(13)	−0.122 (9)	−0.12 (1)	−0.037 (6)	6 (3)	H(26)	−0.386 (8)	0.03 (1)	0.281 (5)	5 (3)
H(14)	−0.204 (9)	−0.38 (1)	−0.038 (6)	5 (3)	H(32)	−0.245 (10)	0.35 (1)	0.255 (7)	8 (3)
H(15)	−0.267 (9)	−0.47 (1)	0.068 (5)	6 (3)	H(33)	−0.421 (8)	0.52 (1)	0.203 (5)	4 (2)
H(16)	−0.226 (8)	−0.31 (1)	0.181 (6)	5 (3)	H(34)	−0.565 (9)	0.42 (1)	0.094 (5)	5 (3)
H(22)	−0.066 (8)	−0.19 (1)	0.324 (6)	5 (3)	H(35)	−0.505 (9)	0.27 (1)	0.012 (6)	6 (3)
H(23)	−0.112 (8)	−0.34 (1)	0.429 (5)	5 (3)	H(36)	−0.401 (8)	0.03 (1)	0.093 (6)	5 (2)
H(24)	−0.287 (8)	−0.31 (1)	0.452 (5)	3 (2)					

[a] The form of the anisotropic thermal parameter is $\exp[-(B_{11}a^{*2}h^2 + B_{22}b^{*2}k^2 + B_{33}c^{*2}l^2)/4 + (B_{12}a^*b^*hk + B_{13}a^*c^*hl + B_{23}b^*c^*kl)/2]$.

Co(II) environment in $CoX_2 \cdot 2P(C_6H_5)_3$ is approximately tetrahedral, the greatest deviation from regular tetrahedral ligand geometry being the X–Co–X angle, which is about 115 and 117° for X = Br and Cl, respectively, i.e., considerably larger than the tetrahedral angle. This may be explained by the mutual repulsion of the halide anions, which are relatively free to move away from each other since in the local CoX_2 plane there are no other atoms present to hinder such a displacement. We remark that the difference of about 0.14 Å between the values for the Co–X bond lengths for X = Cl and Br in Table II may be attributed to the difference in ionic radii of the Cl and Br ions.

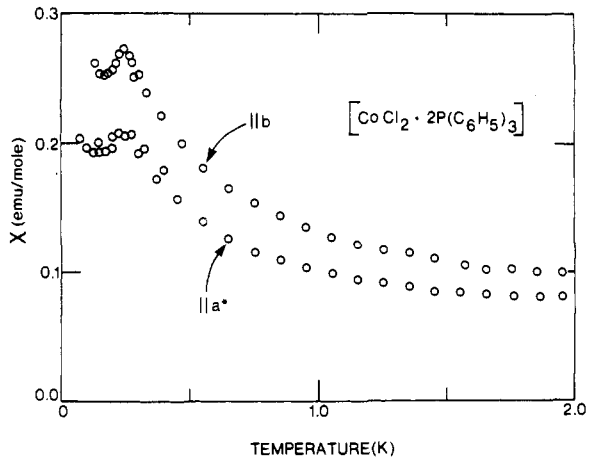

Figure 4. Susceptibilities parallel to the a^* and b axes of $CoCl_2 \cdot 2P(C_6H_5)_3$.

Table II. Bond Lengths and Intermolecular Distances (Å) for $Co[P(C_6H_5)_3]_2Cl_2$ (A) and $Co[P(C_6H_5)_3]_2Br_2$ (B)

	A	B		A	B
Co-X[a]	2.212 (1)	2.349 (2)	⟨C-C⟩[b]	1.382 (2)	1.380 (5)
Co-P	2.384 (1)	2.385 (2)	⟨C-H⟩[b]	1.01	0.95
P-C(11)	1.822 (1)	1.820 (3)	X-C(15)	3.550 (3)[c]	3.591 (5)[c]
P-C(21)	1.827 (1)	1.818 (4)			
P-C(31)	1.825 (1)	1.824 (3)			

[a] X = Cl, Br. [b] Average value. [c] $-x$, $1 + y$, $^1/_2 - z$.

Susceptibility Measurements. The temperature dependences of the susceptibilities parallel to the c axes of both compounds are presented in Figure 3. Broad maxima are found at about 0.37 K for the chloride and 0.52 K for the bromide. At lower temperatures, the susceptibilities decrease toward zero, which may be interpreted in terms of long-range antiferromagnetic ordering, the c axis being the easy or preferred axis of spin alignment in both compounds. The ordering temperature as derived from the maximum slope of the χ vs. T curve is 0.21 ± 0.01 K for the chloride, while the bromide orders at 0.25 ± 0.01 K. The susceptibilities parallel to the a^* and b axes of $CoCl_2 \cdot 2P(C_6H_5)_3$ are displayed in Figure 4; the a^* axis is defined as perpendicular to both the b and the c axes. The data rise to a maximum at about 0.25 K and then appear to go through a shallow minimum at the lower temperatures.

Specific Heat Measurements. The specific heats of both compounds are presented in Figure 5 (on a reduced temperature scale). No lattice (phonon) contribution was observed below 1 K. The ordering temperatures are 0.22 ± 0.005 and 0.26 ± 0.005 K for the chloride and bromide, respectively, in good agreement with those found from the susceptibility measurements. Furthermore, the entropy found by taking the integrals $\int (C/T)\, dT$ for both salts equals R ln 2 within the experimental errors of about 2%. This indicates that the Co^{2+} ion is in an effective spin $S' = {}^1/_2$ state in the temperature range ($T < 1$ K) covered in the experiments.[9]

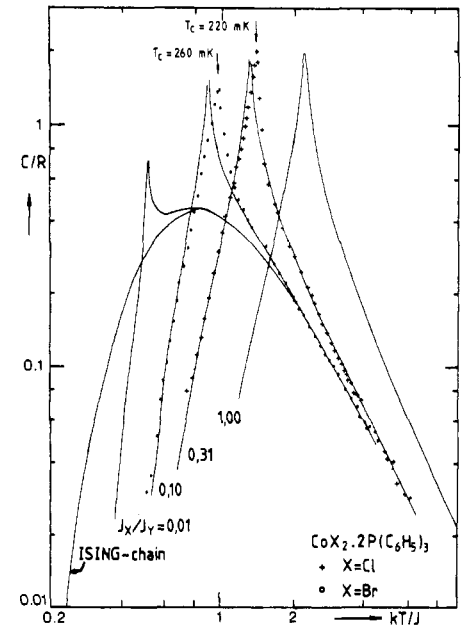

Figure 5. Measured specific heats of $CoCl_2 \cdot 2P(C_6H_5)_3$ (+) and $CoBr_2 \cdot 2P(C_6H_5)_3$ (●). The curves are explained in the text. The interaction constants, J, used in obtaining the relative temperature scales are defined by $|J| = |J_y|$.

Discussion

We consider the susceptibility data sets for the chloride as typical of those expected for the susceptibilities measured parallel and perpendicular to the easy axis of an ordered antiferromagnet with strong, uniaxial, Ising type of anisotropy. Note especially the reduced magnitude of the perpendicular susceptibilities in comparison with those measured along the c axis. These results confirm the picture of the magnetic interactions in this compound, which will be presented below, so that it was not considered necessary to measure the susceptibility in the perpendicular directions for the isostructural bromide. As regards an anisotropy in the strength of the interaction along the various crystallographic directions, we point out that the broad susceptibility maxima as well as the pronounced high-temperature tails of the specific heat curves are indicative of a low-dimensional magnetic lattice. We will now show that this may indeed be anticipated from the superexchange paths connecting Co^{2+} ions within the crystallographic structure.

A projection of the structure of $CoX_2 \cdot 2P(C_6H_5)_3$ onto the ac plane is presented in Figure 6. The large triphenylphosphine ligands, which are not expected to provide a good superexchange path, effectively separate the metal ions in the a direction. On the other hand, a much more favorable Co–X···X–Co superexchange path, albeit long, is apparent in the figure along the c axis.

Table III. Bond Angles (Deg) for $Co[P(C_6H_5)_3]_2Cl_2$ (A) and $Co[P(C_6H_5)_3]_2Br_2$ (B)

	A	B		A	B
X-Co-X'	117.28 (3)	115.24 (3)	P-C(11)-C(12)	117.8 (1)	118.2 (3)
X-Co-P	107.23 (1)	105.03 (3)	P-C(11)-C(16)	122.9 (1)	122.8 (3)
X-Co-P'	104.85 (1)	107.27 (3)	P-C(21)-C(22)	119.3 (1)	118.5 (3)
P-Co-P'	115.88 (2)	117.45 (5)	P-C(21)-C(26)	121.9 (1)	123.2 (3)
Co-P-C(11)	114.09 (4)	114.8 (1)	P-C(31)-C(32)	117.9 (1)	118.6 (3)
Co-P-C(21)	117.10 (4)	117.1 (1)	P-C(31)-C(36)	122.2 (1)	121.2 (3)
Co-P-C(31)	109.39 (5)	109.7 (1)	⟨C-C-C⟩[a]	120.0	120.0
C(11)-P-C(21)	104.89 (6)	104.8 (2)			
C(11)-P-C(31)	105.14 (6)	104.8 (2)			
C(21)-P-C(31)	105.25 (6)	104.6 (2)			

[a] Average C-C-C angle for phenyl carbons.

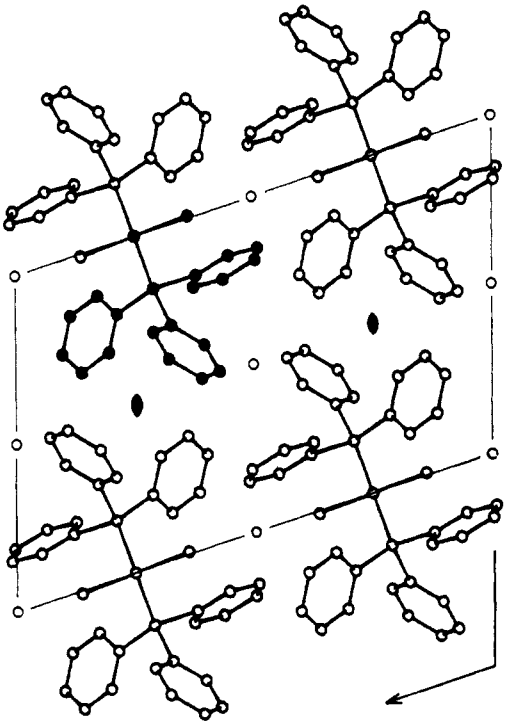

Figure 6. Projection of the structure of $CoX_2 \cdot 2P(C_6H_5)_3$ onto the *ac* plane. The asymmetric unit is indicated by filled circles. Molecules with the metal atom at $y = {}^1/_4$ are related to molecules with $y = {}^3/_4$ by inversion centers.

Since the bulky triphenylphosphine groups are expected to hinder exchange interaction along the *a* axis, one expects at most two-dimensional magnetic behavior. Indeed, examination of a projection of the structure onto the *bc* plane (Figure 2) even suggests that important one-dimensional magnetic character may be present, with the magnetic chains running along the *c* axis in the zigzag fashion indicated by the broken lines in Figure 2. Namely, the Cl–Cl distances along these broken lines are considerably smaller (5.535 (2) Å) than the Cl–P distances (minimum 6.439 (3) Å) connecting Co^{2+} ions along the *b* direction. The corresponding distances in $CoBr_2 \cdot 2P(C_6H_5)_3$ are 5.379 (3) Å for Br–Br and 6.469 (4) Å for Br–P. Thus, the Br–Br distance is actually shorter than the corresponding Cl–Cl distance. Magnetic ordering in less than three dimensions is also suggested by the ratio $T(\chi_{max})/T_c$, which is 1.8 (Cl^-) and 2.1 (Br^-). These values are typical of those found for ordering in lower dimensions.[22]

The anisotropy in the susceptibility is explained as follows. If the $|\pm{}^3/_2\rangle$ doublet of the $^4A_2$ manifold is the ground state, this yields a highly anisotropic effective spin $S' = {}^1/_2$ system, with $g_{\parallel} = 3g_{\parallel} \approx 7.2$ and $g_{\perp} \approx 0$.[5,10,23] One therefore expects an Ising type exchange interaction, and this is consistent with the large anisotropy displayed by the measured susceptibilities of $CoCl_2 \cdot 2P(C_6H_5)_3$. In agreement with the above considerations, the data have been fit most successfully by using the recent calculations for the susceptibility of the rectangular (or anisotropic two-dimensional) Ising lattice with spin $S = {}^1/_2$ of Tanaka and Uryû.[24] The Hamiltonian they use is, for the *g*th spin

$$\mathcal{H}(\sigma_g) = -\sum_{\rho} J_\rho \sigma_{g+\rho} \sigma_g - g\mu_B H \sigma_g$$

where $\sigma(=\pm 1)$ is the Pauli spin operator, ρ is the lattice vector, J_ρ is the exchange-interaction constant, and H is the external magnetic field. A quadratic magnetic lattice is defined as one in which the exchange constants in a plane, J_x and J_y, are equal. For Ising type interactions a transition to long-range magnetic order can occur in such a system.[25] As lattice anisotropy is introduced, a rectangular magnetic lattice is obtained ($J_x \neq J_y$). The limit $J_x \rightarrow 0$ yields the isolated Ising linear chain. In that case, only a broad maximum is obtained in the specific heat, since long-range order can no longer occur. The solid curves in Figures 3 and 5 are best fits of this model to the susceptibility and specific heat data and agree quite well. For the chloride, the best-fit parameters to the theory of Tanaka and Uryû for the susceptibility are $J_x/k_B = 0.046 \pm 0.002$ K, $J_y/k_B = 0.150 \pm 0.005$ K, $J_x/J_y = 0.31 \pm 0.02$, and $g_c = 7.33 \pm 0.10$. For the bromide, these parameters are $J_x/k_B = 0.026 \pm 0.005$ K, $J_y/k_B = 0.265 \pm 0.002$ K, $J_x/J_y = 0.10 \pm 0.02$, and $g_c = 7.22 \pm 0.10$.

The analysis of the specific heat is presented in Figure 5, together with the data. Solid curves represent the calculated specific heats for rectangular Ising systems having different J_x/J_y values; calculations were done according to the theory of Onsager.[25] Curves for the linear chain and quadratic planar lattice are also illustrated.

The ratios $J_x/J_y = 0.31$ (Cl) and 0.10 (Br) give good fits to the data, except near the critical point. We attribute these deviations to the effect of interlayer interactions, i.e., to three-dimensional interactions between the *bc* planes. It proved to be difficult to reconcile theory and experiment for other values of the ratio J_x/J_y. Thus these systems actually lie closer to being one-dimensional antiferromagnets rather than two-dimensional ones, and the bromide compound is more one-dimensional than is the chloride. This must be due to the larger size of bromide and the shorter Br–Br distance illustrated in Figure 2.

In conclusion, we note that these systems provide quite interesting examples of the rectangular Ising model. Although the magnitude of the zero-field splitting cannot be determined from the present data, its negative sign is established without doubt. This leaves the $|\pm{}^3/_2\rangle$ doublet as the ground state, and the specific heat data indicate that the $|\pm{}^1/_2\rangle$ state is already sufficiently depopulated at temperatures below 1 K so as not to affect significantly the thermodynamic behavior.

Acknowledgment. We thank Dr. Uryû for providing details of the calculations in ref 24 and Professor W. J. Huiskamp for his interest in this work and a critical reading of the manuscript. This research was supported by the National Science Foundation through Grants DMR77-13318 and DMR7906119 in Chicago and CHE77-01372 in Charlottesville. This work is part of the research program of the "Stichting voor Fundamenteel Onderzoek der Materie (FOM)", which is financially supported by the "Nederlandse Organisatie voor Zuiver-Wetenschappelijk Onderzoek (ZWO)".

Registry No. $CoCl_2 \cdot 2P(C_6H_5)_3$, 14126-40-0; $CoBr_2 \cdot 2P(C_6H_5)_3$, 14126-32-0.

Supplementary Material Available: Listings of observed and calculated structure factors (19 pages). Ordering information is given on any current masthead page.

(22) de Jongh, L. J.; Miedema, A. R. *Adv. Phys.* **1974**, *23*, 1.
(23) Carlin, R. L.; van Duyneveldt, A. J. "Magnetic Properties of Transition Metal Compounds"; Springer-Verlag: New York, 1977; p 204.
(24) Tanaka, Y.; Uryû, N. *Phys. Rev. B: Condens. Matter* **1980**, *21*, 1994.
(25) Onsager, L. *Phys. Rev.* **1944**, *65*, 117.